

Effect of Angle Ply On The Mechanical Performance of Jute Fibre Woven Mat /Epoxy Composites With Varying Ageing Conditions

Satheeshkumar S.

Kongu Engineering College

Sathishkumar T. P

Kongu Engineering College

Rajini Nagarajan (✉ rajiniklu@gmail.com)

Kalasalingam Academy of Research and Education <https://orcid.org/0000-0002-2337-3470>

Navaneethakrishnan P.

Kongu Engineering College

Sikiru O. Ismail

University of Hertfordshire

Suchart Siengchin

King Mongkut's University of Technology

Faruq Mohammad

King Saud University

Hamad A. Al-Lohedan

King Saud University

Research Article

Keywords: Jute fiber mat, layering patterns, polymer composites, mechanical properties, Fick's law, Arrhenius principle, service life.

Posted Date: September 29th, 2021

DOI: <https://doi.org/10.21203/rs.3.rs-919614/v1>

License:  This work is licensed under a Creative Commons Attribution 4.0 International License.

[Read Full License](#)

Effect of angle ply on the mechanical performance of jute fibre woven mat /epoxy composites with varying ageing conditions

S. Satheeshkumar¹, T. P Sathishkumar^{1*}, N. Rajini^{2*}, P. Navaneethakrishnan¹,
Sikiru O. Ismail³, Suchart Siengchin⁴, Faruq Mohammad⁵, Hamad A. Al-Lohedan⁵

¹Department of Mechanical Engineering, Kongu Engineering College, Perundurai, Erode,
Tamilnadu, India

² Department of Mechanical Engineering, Kalasalingam Academy of Research and Education,
Krishnankoil 626126, Tamilnadu, India.

³Department of Engineering, School of Physics, Engineering and Computer Science, University
of Hertfordshire, Hatfield, AL10 9AB, Hertfordshire, England, United Kingdom.

⁴Department of Materials and Production Engineering, The Sirindhorn International Thai-
German Graduate School of Engineering (TGGGS), King Mongkut's University of Technology
North Bangkok, 1518 Wongsawang Road, Bangsue, Bangkok 10800, Thailand.

⁵Department of Chemistry, College of Science, King Saud University, P.O. Box 2455, Riyadh,
Kingdom of Saudi Arabia 11451.

*Corresponding authors: N. Rajini, E-mail: rajiniklu@gmail.com and T. P. Sathishkumar, E-
mail: tpsathish@kongu.ac.in, Tel.: +91 9943570495

Abstract

The present work investigates the mechanical strengths retention and prediction of maximum service life of sets of laminated composites by analyzing their diffusion coefficients and activation energies, using Fick's law and Arrhenius principle. Jute fiber woven mat reinforced epoxy laminated composites (JFMRLCs) were prepared by simple hand lay-up and compression molding methods. The layering patterns of 0° balanced laminate of [0°/0°/0°/0°/0°], 30° angle-ply laminate of [0°/+30°/0°/-30°/0°] and 45° angle-ply laminate of [0°/+45°/0°/-45°/0°] were used to prepare the composite samples, according to classical laminated plate theory (CLPT). The composites were immersed in water at different periods of 10, 20, 30 and 40 days aging. The effects of the various periods of aging on their mechanical properties were studied.

The results showed that the weights of the composite samples increased by increasing the aging periods. The mechanical properties of aged (wet) composites were compared with the unaged (dry) counterparts to predict their strengths retention. The composite with 45° layering pattern exhibited the maximum strength retention. Also, the same composite sample with layering pattern of 45° produced the maximum activation energy, based on Arrhenius principle. The tensile fractured surfaces were analyzed to investigate into their fiber-matrix interfacial bonds through images obtained from scanning electron microscopy (SEM). Summarily, it was evident that optimum JFMRLCs with layering pattern of 45° exhibited best mechanical properties. Hence, they can act as suitable, sustainable, low cost and environmentally friendly composite materials for structural marine and other related engineering applications.

Keywords: Jute fiber mat, layering patterns, polymer composites, mechanical properties, Fick's law, Arrhenius principle, service life.

1. Introduction

Natural fibers have been traditionally used for preparing roof sheets and ropes, due to their availability, strength, lightweight and ease of extraction from plants [1]. Today, the material scientists are continuously searching for reusable, renewable and biodegradable materials for automobile [1-3], construction [4,5] and packaging applications [6] for the last two decades. The natural fiber reinforced polymer composites (NFRPCs) have been widely used for various semi-structural and structural applications, due to their lighter weights when compared with synthetic fiber reinforced polymer composites [7-9]. The wider use of NFRPCs can be attributed to the ease of their manufacturing, less processing cost, abundant availability, non-toxicity and environmentally friendliness, among other factors [10-13]. Furthermore, the need for lightweight materials for various structural applications in order to reduce the total weight of structures and quantity of carbon dioxide (CO₂) is increasing. Various types of NFRPCs are highly demanded by the construction, aviation and automobile industries. NFRPCs are developed using various fibers, such as jute, sisal, hemp, snake grass, banana, to mention but a few [14].

In addition, it is very important to investigate into mechanical properties of the NFRPCs, including tensile, flexural, impact and fatigue before they are used. The choice of properties depends on their specific areas of applications. Also, tests are often carried out to optimize the fiber volume or weight fractions, fiber length and fiber orientation, which mainly determine the mechanical behaviors of the NFRPCs [15-17]. For building construction, asbestos, galvanized steel and plastic roof sheets have been used for roofing for the past seven decades. The use of asbestos sheets increase the total weight of the structure, handling of galvanized sheets has higher risk and cost, and plastic sheet attracts higher cost. Also, toxic gasses emit during the production of these sheets, damaging the environments. Alternatively, NFRPCs are widely used for roofing application recently to avoid the aforementioned problems. The roof sheets are developed into various shapes according to end users' request, using various natural fibers. Therefore, the square and rectangular shapes NFRPC sheets are used for various building parts, such as roofs, side walls and garden desks. The development of NFRPC sheets with jute fiber yarn mats has supported the concept of light weighting of structure and offered environmentally friendliness to the environments [6-8].

However, NFRPC sheets can absorb moisture during rainy and high humidity seasons. Due to this drawback, the durability and long-term sustainability are reduced with their mechanical properties and fiber-matrix interfacial bonding [18-20]. Therefore, moisture absorption, mechanical properties retention, diffusivity and service life of materials must be analyzed before using NFRPC sheets for various applications. For instance, an increase in moisture absorption reduced both tensile and flexural strengths of jute fiber reinforced polyester composites at 25 and 100 °C of de-ionized water on different periods [16]. The rate of degradation of these composites was found higher at 100 °C. Increasing the number of jute fiber mat and aging period gradually increased the weight of the composites. At fiber volume fraction of 21%, the dry composites showed higher mechanical properties than the wet composites. The untreated, alkali and silane treated jute fiber composites depicted higher tensile strengths than the untreated basalt fiber composites. Addition of alkali and silane treated jute fibers to the composites reduced the

moisture absorption. The tensile strength retention was observed higher for composites aged at normal water when compared with alkali aged composites [17,21,22].

Moreover, the long-term performance of flax fiber reinforced polymer (FRP) composites was compared with glass FRP composite specimens [23]. The specimens were exposed to dry heat, distilled, salt and alkaline water with different temperatures of 20, 50 and 60 °C. Their tensile properties reduced by increasing the aging temperature and period. The flax FRP composites showed tensile strengths retention of 23% higher than the glass FRP composites. The weight gains of flax FRP composites was obtained higher than glass FRP composites. Similar study reported that the mass loss decreased as functions of both temperature and moisture absorption [24]. Incorporation of glass fiber to *Pennisetum purpureum*/natural fiber epoxy composites enhanced their mechanical properties and then reduced their water absorption [25]. The wet composites showed less tensile and flexural strengths when compared with dry composites.

Besides, NFRPCs can replace the glass FRP composites, due to their less weight, easily availability, ease of handling/tailoring and biodegradability [26]. The mechanical properties retention and service life of glass fiber pultruded composites were examined at different periods and environmental conditions. The tensile and flexural strengths deceased by increasing the aging period, due to an increase in the diffusion coefficients of the aged composites. The Arrhenius principle was used to predict the service life of the FRP composites [27-29]. The moisture absorption of natural and synthetic FRP composites can reduce their mechanical properties and service life [30-32]. The use of NFRPCs for various structural applications is increasing rapidly, because it can significantly reduce the total structural weight on component or system [33].

Based on the afore-reported works among others, it is evident that study on general mechanical properties of jute fiber mat reinforced polymer composites has not been comprehensively investigated, especially for structural applications. Precisely, the study on their long-term service life and mechanical properties is highly germane for effect utilization of jute fiber mat reinforced polymer composites for various lightweight structural application. Hence, this present work aimed to prepare three different layering patterns or orientations of jute fiber yarn mat reinforced

epoxy laminated composites (JFMRLCs), using compression molding technique. The composites were immersed in water for long periods to investigate into the effects of jute fiber mat orientations on their mechanical properties retention, diffusivities and activation energies. These were carried out to predict their service life, using Fick's law and Arrhenius principle, as required prior to their various structural applications in a real scenario.

2. Materials and methods

2.1. Fiber and resin

Fig. 1 shows the jute fiber yarn woven mats (JYMs) used to prepare the laminated epoxy composites. The jute fibers were extracted from jute stem by water and manual retting methods, before they were dried for 2 days. The extracted jute fibers were used to prepare the jute fiber yarn by hand spinning process. The hand weaving method was used to fabricate the jute fiber yarn mat with liner density of 6 yarns per square centimeter in warp and weft directions. The thickness of the mat was approximately 1.17 mm. The laboratory grade LY556 epoxy and grade HY951 hardener were used. They were purchased from Covai Senu Industry, Coimbatore, Tamilnadu. Table 1 presents properties of the epoxy resin.

2.2. Composites manufacturing and aging

The laminated composite plates were prepared by reinforcing the epoxy resin with the JYMs. According to classical laminated plate theory (CLPT), the three layering patterns or orientations considered were $[0^\circ/0^\circ/0^\circ/0^\circ/0^\circ]$ balanced laminate, $0^\circ/-30^\circ/0^\circ/+30^\circ/0^\circ$ and $0^\circ/-45^\circ/0^\circ/+45^\circ/0^\circ$ angle-ply laminate, as shown in Figs 1(a), (b) and (c), respectively. They were used to prepare the laminated composites by hand lay-up method with compression molding process. Fig. 1(d) shows the JYM. The epoxy and hardener were mixed by 10:1 ratio, using mechanical stirrer for 20 minutes when preparing the resin solution. A steel mold was used for preparation of the composites. Few manufacturing steps were used to achieve the perfect lamination, ensure the perfect distribution of resin and avoid air bubble formation between the laminas: Step 1 – Releasing agent of polyvinylchloride was applied in die side of the mold surface; Step 2 – A

brush was used to apply the resin solution on surface of the inside part of the mold and placed JYM on applied reins in the mold; Step 3 – Using brush, the reins was applied on the JYM; Step 4 – A roller was rolled over the mat to remove the air bubbles over the mold surface. The aforementioned steps 2, 3 and 4 were repeated to place the next layer of JYMs. After that, the closed mold was kept in a hydraulic press for solidification at pressure of 35 bar and room temperature for 6 hours. The cured composite plate was removed, and post heated in a hot air woven for 3 hours at nearly 45 °C. The holding period and temperature for curing of the composite were provided by the resin supplier. A total of five layers of JYM was used to prepare the laminated composites and obtain thickness of around 7 mm. Four steel plates of $10 \times 10 \text{ mm}^2$ square with 7 mm thick was placed on four corners of the mold to maintain uniform thickness over the composite plates. The dimensions: length, width and thickness of the laminated composite plates were 240, 200 and 7 mm, respectively. The composite samples were immersed in a three sets of plastic bowls of water for 10, 20, 30 and 40 days, as previously depicted in Fig. 1(e).

2.3. Tensile testing

Tensile samples were cut by using a zig-zag cutter according to ASTM D638 standard [33,34]. The shape of specimens was in dog-bone with dimensions: length, width and thickness of 165, 19 and 7 mm, respectively. Universal testing machine: DEEPAK poly plastic Pvt, DX 25 kN with load cell of 25 kN was used to perform the tensile test and obtain the tensile stress, strain and molds from the recorded load *versus* elongation curves. The load cell was used to measure the load and encoder was used to measure extension of the samples. The crosshead speed of test was 2 mm/min and the test was conducted at room temperature. The gauge length and width at gauge length of the specimen were 50 and 13 mm, respectively. A total of five identical composite samples were tested and average values were plotted. Fig. 2 shows the tensile fractured specimens, as all samples broken between the gauge length after test.

2.4. Flexural testing

The flexural test samples were cut from the composite plates according to ASTM D790 standard. The shape of specimens was in rectangular and thickness of each sample was 7 mm. The span-to-depth ratio was 16:1. The same universal testing machine, namely DEEPAK poly plastic Pvt, DX25 kN with 500 N load cell was used to perform the flexural test with cross head speed of 1.5 mm/min and obtain the flexural stress, strain and modulus, using Eqs (1), (2) and (3), respectively [33,34]. Similarly, a total of five identical flexural samples were tested for three composites and average values were taken for discussion. Fig. 3 shows the fractured specimens from flexural test. The following Eqs (1)-(3) were used to calculate the flexural properties of the various composite samples.

$$\sigma$$

$$= \frac{3PL}{2bd^3} \quad (1)$$

Where, σ = flexural stress in MPa, P = peak load in N, l = span length in mm, b = width of sample in mm, d = depth of sample in mm, and

$$e = 6Ed/L^2$$

(2)

Where e = flexural strain in percentage (%), and E = extension in mm, also:

$$E_B$$

$$= \frac{L^3 m}{4bd^3} \quad (3)$$

Where E_B = modulus of elasticity in GPa and m = slope of the tangent to the initial straight-line portion of the load-deflection curve in N/mm of deflection.

2.5. Impact testing

Similar to other test samples, impact test samples were cut from the composite plates. Impact test was conducted on test sample size of $64.0 \times 12.7 \times 7.0$ mm³, according to ASTM D-256 standard. Impact testing machine, known as IZOD TESTC-R, Deepak poly-Plast Pvt. Ltd was used. The load cell of drop weight hammer and machine accuracy were 25 and 0.001 J,

respectively. Before testing, the manually-operated notch cutter was used to make the V-notch on the specimens. Similar to other tests, a sum of five identical samples were tested for three composite samples and average values were plotted. Fig. 4 shows the impact fractured specimens after the test.

2.6. Aging of laminated composites

The aging process of composite specimens was done in accordance with ASTM D570-98 standard [29,30]. The laminated composite specimens were immersed in normal water to conduct the natural aging, as previously shown in Fig. 1(e). Before aging, the digital weight measuring machine with accuracy of 0.001 gram was used to obtain the weights of all dry samples. Frequently, the weights of all aging specimens were obtained at regular interval of 5 days and recorded for analysis. Total duration of immersion was 40 days. Before weighting, all samples were dried using a paper and again immersed in water. The tensile, flexural and impact samples were aged and their weights were obtained before various mechanical testing.

Besides, the percentages of weight gains (Δ_m) [16,17,27,28,35] with respect to the unaged composite specimens were calculated, using Eq. (4).

$$\Delta_m = \left(\frac{m_t - m_0}{m_0} \right) \times 100$$

(4)

Where, m_t = weight of the composite sample (gram) at time t and m_0 = weight of the composite sample at initial state (gram). Based on Fick's law, the apparent diffusion coefficient, D in Eq. 5 was calculated by considering the aging process [27,28].

$$D = \pi \left(\frac{h}{4M_m} \right)^2 \left(\frac{M_2 - M_1}{\sqrt{t_2} - \sqrt{t_1}} \right)^2 \left(1 + \frac{h}{l} + \frac{h}{n} \right)^{-2} \quad (5)$$

Where, h , l and n = thickness, length and width of the JFMRLC sample (mm) respectively, M_m = maximum moisture absorption of the JFMRLC sample (gram), M_1 and M_2 = moisture absorption (gram) of the JFMRLC sample at times t_1 and t_2 (sec), respectively.

Therefore, the activation energy was calculated, using Arrhenius principle [27,28]; according to Eq. 6.

$$k = Ae^{\left(\frac{-E_a}{RT}\right)} \quad (6)$$

Where A = pre-exponential factor, T = temperature (Kelvin), E_a = activation energy (kJ/mol) and R = Boltzmann constant (usually 1.38065×10^{-23} J/Kelvin).

2.7. Scanning electron microscopy

The morphology of each of the tensile fractured laminated composite sample was examined. Scanning electron microscopy (SEM) images were obtained and used to analyze their fiber-matrix interfacial bonding and micro structural failure. The following SEM machine specifications were used for scanning or imaging: resolution of 3.0 nm (Acc. V 15 kV and WD 8 to 9 mm), magnification of 50 to 500x and electron gun accelerating voltage of 0.5 to 30 kV. Before imaging, the fractured samples were cut into length of 5 mm and golden coated to improve their conductivity and resolution.

3. Results and discussion

3.1. Weight variation

Fig. 5 shows the percentage of weight gain *versus* aging period of JFMRLCs with different orientations of jute fiber mats. Eq. 4 was used to calculate the percentage of weight gain [4,8]. Once in every five days, the composite samples were taken out from the plastic bowl (Fig. 1e) and their weights were measured to calculate the percentages of weight gains.

Fig. 5(a) shows the weight gains of tensile samples at different aging periods and fiber mat orientations. The percentage of weight gain increased with the aging period. The composite with 0° and 30° layering patterns of JYM showed lower water gain than 45° layering pattern. Up to

30 days, the weight gains by the composites with 0° and 30° orientations gradually increased. After every five days aging and up to 40 days, the weight gains of the composites reached fullness. At 45° layering pattern, the composite reached maximum water gain at 35 days. The higher weight gain was observed from tensile sample with 45° layering pattern of JYM. Fig. 6 shows both dry and wet fiber surfaces. The dimension of dry fiber was lower than the wet fiber (Fig. 5a). It was observed that the fiber surface was swelled, due to continuous absorption of water for longer period of 40 days. The swelling consequently reduced the fiber-matrix physical bonding. Therefore, the fiber load carrying capacity reduced with their mechanical properties. The percentage differences of weight gains between 35 and 45 days were 1.14, 1.19 and 1.01% at 0°, 30° and 45° layering patterns, respectively. The percentage improvement of weight gain was very minimum, which supported the composite to reach maximum water absorption. The percentage differences of weight gains between orientations at maximum water absorption and 40 days were 3.51, 13.64 and 17.65% from 0° to 30°, 30° to 45° and 0° to 45°, respectively.

Similarly, Fig. 5(b) shows the weight gains of flexural samples at different periods and fiber mat orientations. The composite with 0° layering pattern of JYM showed lower water gain than both 30° and 45° layering patterns. Up to 20 days, the weight gain by composites gradually increased. Continuous swelling up to 40 days was observed, as the weight gains by the composites reached maximum. The higher weight gain was observed from the flexural samples with reinforcement of 45° layering pattern. The percentage differences of weight gains between 35 and 45 days were 1.90, 1.47 and 0.86% at 0°, 30° and 45° layering patterns, respectively. The percentage improvement of weight gain was very minimum, which supported the composite to exhibit minimum water absorption. The percentage differences of weight gains between orientations at maximum absorption for 40 days were 5.78, 5.45 and 10.91% from 0° to 30°, 30° to 45° and 0° to 45°, respectively.

Also, Fig. 5(c) shows the weight gains of impact samples at different periods and fiber mat orientations. The percentage of weight gain increased with the aging period. The composite with 0° layering pattern of JYM always showed lower water gain than the 30° and 45° layering patterns. Up to 25 days, the weight gain of composites gradually increased at 0° orientations. After every five days aging till up to 40 days, the weight gains by the composites reached maximum. At 30° and 45° layering patterns, the maximum water gain was obtained in 35 days. The higher weight gain was recorded for tensile sample reinforced with 45° layering pattern of JYM. The percentage differences of weight gains between 35 and 45 days were 0.49, 1.82 and 1.78% at 0° , 30° and 45° , respectively. The percentage improvement of weight gain was very minimum, which caused the composite to exhibit minimum water absorption. The percentage differences of weight gains between orientations at maximum absorption for 40 days were 5.668, 1.780 and 7.540% from 0° to 30° , 30° to 45° and 0° to 45° , respectively. However, the maximum water gain was obtained from composite sample with 45° layering pattern of JYM.

3.2. Tensile properties

Fig. 7 shows the tensile stress-strain curves of dry and aged (wet) JFMRLCs at different layering patterns of 0° , 30° and 45° as well as periods of 10, 20, 30 and 40 days. The tensile stress was plotted by considering the average values of loads of five samples and areas of cross sectional areas of the samples. The width of dog-bone shape of the specimen over the gauge length of 50 mm was taken as 13 mm. Figs 7(a), (b) and (c) show that the slope of the curves was linearly increased. The tensile stress curve of dry JFMRLC with 0° layering pattern was higher when compared with 30° and 45° layering patterns. From this test, the specimens of different layering samples indicated that the stress *versus* strain curve decreased gradually by increasing aging days. The slope of aged composites changed by varying the layering pattern and period of immersion. Fig. 8 shows the tensile properties of JFMRLCs. The tensile stresses of dry samples were 34.04, 31.97 and 29.36 MPa at 0° , 30° and 45° layering patterns, respectively. The tensile strains of dry samples were 2.74, 2.64 and 2.42% at 0° , 30° and 45° layering patterns,

respectively. The tensile moduli of dry samples were 1.24, 1.21 and 1.21 GPa at 0°, 30° and 45° layering patterns, respectively.

In addition, at 0° layering pattern, the tensile strengths of the wet samples were lower than that of dry composites. At 10 days aging, the composites showed higher tensile properties (Fig. 8a) when compared with wet composites of other two layering patterns. At 20, 30 and 40 days aging, the composite showed lower tensile strengths when compared with wet composites of 30° and 45° layering patterns. The tensile strengths of composite samples with 0° layering pattern were 29.87, 23.45, 21.61 and 18.55 MPa; tensile strains of 2.74, 2.74, 2.64 and 2.10%; tensile moduli of 2.14, 1.09, 0.85 and 0.88 GPa at 10, 20, 30 and 40 days aging, respectively. The tensile moduli gradually decreased with increasing aging periods. The reduction in percentages of tensile strengths between dry and wet composites were 12.25, 31.11, 36.52 and 45.51% at respective 10, 20, 30 and 40 days aging, as depicted in Fig. 8(a). Increasing the aging period gradually reduced the tensile strengths and moduli of the composites (Fig 9a), due to absorption of moisture by the fiber/JYM. Due to presence of moisture, the rate of tensile strength reduction gradually increased at 0° layering pattern. The reduction was faster than that of 30° and 45° layering patterns. Fig. 9(b) shows the tensile strengths retention.

Moving forward, the dry fiber reinforced composites (Fig. 10a) exhibited highest mechanical properties than the wet fiber counterparts (Fig. 10b), because the fiber surfaces did not swell and the higher fiber surface roughness supported higher fiber-matrix interfacial bonding. The wet fiber in the composite systems showed micro biodegradable failure (Fig. 10c) when compared with occurrence of shear failure and debonding between dry fiber and matrix, as shown in Figs 10(d), (e) and (f). It can also be observed that the dry fiber surface, after pulled out from composites, showed many micro scratches, as depicted in Figs 10(g) and (h). This resisted the fiber pull-out, which increased the mechanical properties of the composites. However, the wet fiber surfaces, after pulled out from their composites, showed swelling effect, as shown in Figs

10(i) and (j). This can easily pull out from the composites, which could reduce their mechanical properties.

Besides, at 30° layering pattern, the tensile strength was higher (Fig. 8b) when compared with all other cases, because of the orientation of the dry fiber and absence of swelling effect on fiber surface (Fig. 10a). The tensile strength of wet composites was higher when compared with wet composites of 0° and 45°layering patterns at 20, 30 and 40 days aging. This can be attributed to the less moisture absorption in the fiber. The tensile strengths of composite samples with 30° layering pattern were 29.02, 26.67, 24.45 and 21.64 MPa; strains of 2.64, 2.74, 2.96 and 2.96%; tensile moduli of 1.10, 0.97, 0.83 and 0.73 GPa at 10, 20, 30 and 40 days, respectively. The tensile modulus gradually decreased by increasing the aging period and when compared with 0° layering patterns, they recorded higher values. The percentages of tensile strengths reduction (Fig. 9a) between dry and wet composites were 9.23, 16.28, 23.52 and 32.31% at 10, 20, 30 and 40 days aging, respectively.

At 45° layering pattern, the tensile strength was higher for dry fiber composites when compared with wet composites (Fig. 8c). The tensile strength of wet composite was lower when compared with all other cases. This can be attributed to the higher moisture absorption and fiber orientation. The tensile strength of composite containing 45° layering pattern were 24.82, 23.48, 22.23 and 20.33 MPa; tensile strains of 2.55, 2.74, 2.42 and 2.42%; tensile moduli of 0.97, 0.86, 0.92 and 0.84 GPa at 10, 20, 30 and 40 days aging. The tensile modulus gradually decreased by increasing the aging period, and when compared with 0° and 30° layering patterns, they recorded lower values. The percentages of tensile strengths reduction (Fig. 8a) between dry and wet composites were 15.46, 20.03, 20.02, 24.28 and 30.60 % at 10, 20, 30 and 40 days aging. From these graphs, the 30° layering pattern showed higher tensile properties than the 0° and 45° layering patterns.

3.3. Flexural properties

The flexural properties were analyzed, using three-point bending test method. Fig. 11 shows the flexural stress- strain curves of dry and aged (wet) JFMRLCs at different layering patterns (0° , 30° and 45°) and periods (10, 20, 30 and 40 days). The flexural stress curves were plotted by using Eqs (1) and (2), considering the average values of loads on five samples into the average value of area of cross section of samples. Fig. 11 shows that the slop of the curves is almost linearly increased at all days. The flexural stress curve of dry JFMRLC was observed higher, when compared with wet/aged JFMRLC. In these curves, the composite of different layering pattern indicates that the stress versus strain curve was gradually decreased by increasing aging days. The slop of aged composites varied by varying the layering pattern and period of immersion. Fig. 12 depicts the flexural properties of JFMRLCs. The flexural stresses of dry samples were 76.52, 78.45 and 96.64 MPa at 0° , 30° and 45° , respectively. The flexural strains of dry samples were 2.28, 1.97 and 2.28% at 0° , 30° and 45° , respectively. The flexural moduli of dry samples were 0.564, 0.629 and 0.614 GPa at 0° , 30° and 45° , respectively.

Furthermore, at 0° layering pattern, the 10 days aging composite showed insignificant higher flexural strength (Fig. 12a) when compared with wet composites at 30° layering patterns. Then, at 20, 30 and 40 days aging, the composite exhibited lower properties when compared with wet composites of 30° and 45° layering patterns. The flexural strengths of composite with 0° layering pattern were 67.45, 62.45, 58.78 and 51.50 MPa; flexural strains of 2.18, 1.97, 1.96 and 1.84%; flexural moduli of 0.539, 0.441, 0.392 and 0.365 GPa at 10, 20, 30 and 40 days aging, respectively. The flexural moduli gradually decreased by increasing the aging period. The percentages of flexural strengths reduction (Fig. 13a) between dry and wet composites were 11.85, 18.39, 23.18 and 32.31% at 10, 20, 30 and 40 days aging, respectively. Increasing the aging period gradually reduced the flexural strengths (Fig. 10a) and moduli of the composites, due to moisture absorption by the fiber/JYM. The jute fiber bulged continuously when the aging period was increasing. Then, the presence of moisture in jute fiber weakened the fiber-matrix interfacial bonding and resultantly caused decrease in their flexural properties. The dry fiber

composites recorded better bonding with matrix; hence, it produced better interface strength. Due to presence of moisture, the rate of flexural strength reduction gradually increased at 0° layering pattern and it was lower than 30° and 45° layering patterns (Fig. 13b).

Moreover, at 30° layering pattern, the flexural strength was higher (Fig. 12b) when compared with 0° layering pattern, but it was lower than 45° layering pattern, because the the flexural stress depended on orientation of the dry fiber. At 40 days aging, the flexural strength was lower when compared with the wet composites of 0° layering pattern. The flexural strengths of the composite with 30° layering pattern were 66.97, 63.44, 56.45 and 47.61 MPa; flexural strains of 2.03, 1.79, 2.03 and 1.91%; flexural moduli of 0.565, 0.551, 0.494 MPa and 0429 GPa at 10, 20, 30 and 40 days aging, respectively. The flexural modulus gradually decreased by increasing the aging period. When compared with 0° layering patterns, they depicted slightly higher value. The percentages of flexural strengths reduction (Fig. 13a) between dry and wet composites were 14.63, 19.13, 28.04 and 39.31% at 10, 20, 30 and 40 days aging, respectively. This reduction was later higher than that of 0° layering patterns.

At 40° layering pattern, the flexural strength of dry fiber composites showed higher values when compared with wet composites (Fig. 12c). The flexural strength of wet composite was lower when compared with to all other composite systems. This can be attributed to higher moisture absorption and difference in fiber orientation. The flexural strengths of composites with 45° layering pattern were 83.18, 70.84, 64.28 and 60.47 MPa (Fig. 12c); flexural strains of 2.35, 2.16, 2.22 and 2.09%; flexural moduli of 0.586, 0.543, 0.524 and 0.479 GPa at 10, 20, 30 and 40 days aging, respectively. The flexural modulus gradually decreased by increasing the aging period. They recorded higher values when compared with 0° and 30° layering patterns. The percentages of flexural strengths reduction (Fig. 13a) between dry and wet composites were 13.93, 26.70, 33.49 and 37.43% at 10, 20, 30 and 40 days aging, respectively. From same Fig. 13, the 30° layering pattern showed higher properties than both 0° and 45° layering patterns.

3.4. Impact properties

The impact properties of both dry and wet JFMRLCs were measured by drop dower impact testing method. The impact strength of a composite material is an important property for structural application. The low velocity impact tester was used to analyze the impact strength. Fig. 14(a) shows the impact strengths of JFMRLCs at different layering patterns and aging periods. The impact strengths of the dry JFMRLCs were higher at all layering patterns, because the interfacial adhesion between the fiber surfaces and matrix was good. This can be traced to less than 0.25% of moisture content in the jute fiber. This moisture content was required to maintain fiber flexibility and stable chemical bonding of fiber structural elements, such as cellulose, hemicellulose, wax and pectin. The impact strengths of dry JFMRLCs were 6.10, 5.31, 5.19 J/m² at 0°, 30° and 45° layering patterns, respectively.

More also, The jute fiber of aged (wet) JFMRLCs swelled by moisture absorption, which weakened the fiber-matrix bonding and consequently decreased their impact strengths when sudden impact force was applied. At 0° layering patterns, the impact strengths of wet JFMRLCs were 5.29, 4.64, 4.41, 4.34 J/m² at 10, 20, 30 and 40 days aging, respectively. The impact strengths were lower when compared with both 30° and 45° layering patterns. The impact strengths retention and reduction are shown in Figs 14(b) and (c), respectively. The percentages of reduction in impact strengths between wet and aged composites at 0° layering patterns (Fig. 14b) were 13.35, 3.98, 27.76, and 28.84 % at 10, 20, 30 and 40 days aging, respectively. The rate of reduction was lower when compared with other two layering patterns, due to lower rate of water inhalation of jute fibers when compared with 30° and 45° layered JYM. At 30° layering patterns, the impact strengths of wet JFMRLCs were 5.11, 4.60, 4.31, 4.19 J/m² at 10, 20, 30 and 40 days aging, respectively. The impact strengths were lower when compared with 0° layering pattern. The percentages reduction of impact strengths between wet and aged composites with 30° layering pattern (Fig. 14b) were 3.77, 13.99, 18.88 and 21.15% at 10, 20, 30 and 40 days aging, respectively. The rate of reduction was higher when compared with 45° layering pattern. At 45° layering patterns, the impact strengths of wet/aged JFMRLCs were 4.98, 4.46, 4.23, 4.13 J/m² at 10, 20, 30 and 40 days aging, respectively. The impact strengths were lower when

compared with both 0° and 30° layering patterns. The percentages of reduction in impact strengths between wet and aged composites with 45° layering pattern (Fig. 14b) were 3.77, 13.99, 18.88 and 21.15% at 10, 20, 30 and 40 days aging, respectively. The rate of reduction was higher when compared with other two layering patterns. The impact strength was lower, due to higher rate of water ingressions by jute fibers. Fig. 14(c) shows the impact strengths retention of the JFMRLCs.

3.5. Predication of apparent diffusion coefficient and activation energy

An increase in aging period caused a decrease in the mechanical properties of the composites, due to their degradation. The degradation of the composite was predicated by calculating the value of diffusion coefficient, which was calculated from aging period and moisture absorption. Eq. (5) was used to determine the diffusion coefficients of the JFMRLCs. Fig. 15 shows the weights of the composites *versus* square root of periods, which was used to measure the values of moisture absorption. These values were measured from curves of linear fitting of regression line for tensile, flexural and impact samples. Table 2 presents the diffusion coefficient of the JFMRLCs.

Additionally, the diffusion coefficients of the tensile, flexural and impact specimens increased by increasing their layering patterns. The rate of moisture absorption increased by increasing the orientation of jute mat in the JFMRLCs. The JFMRLCs with 45° layering pattern produced maximum degradation. The percentage differences of diffusion coefficients between layering patterns were 2% (0° to 30°), 5.55% (0° to 30°) and 7.69% (0° to 45°) for tensile samples, 3.31% (0° to 30°), 2.29% (0° to 30°) and 5.67% (0° to 45°) for flexural samples, 7.96% (0° to 30°), 7.38% (0° to 30°) and 16.37% (0° to 45°) for impact samples.

Using diffusion coefficients, the activation energies were calculated to establish retention of their mechanical properties and lower rate of degradation of composites. They were determined by using Eq. (6). Table 2 presents the activation energies of tensile, flexural and impact samples

of the JFMRLCs. The higher values of their activation energies showed lower rate of material degradation, which could have higher service life. From the tensile sample results obtained, composite samples with 45° layering pattern exhibited higher activation energy and higher tensile strength up to 30 days aging. Even though, these values were very close, but percentage differences between them were very small. In addition, similar trends were observed from both flexural and impact test sample results. Hence, static (tensile and flexural testing) and dynamic (impact) loading samples exhibited similar trend of activation energy. Therefore, the processes of testing and analyzing their mechanical properties along with validation of diffusion coefficients and activation energies for the JFMRLC material degradation were correct procedures for prediction of service life of the composite materials.

4. Conclusion

JFMRLCs were prepared by compression molding process followed by hand lay-up method of manufacturing jute fiber mat at 0° , 30° and 45° layering patterns. The composites were aged for 10, 20, 30 and 40 days to analyze the mechanical properties retention and calculate their diffusion coefficients and activation energies for prediction of maximum service life. The mechanical strengths retention of JFMRLCs were higher at 45° layering pattern for all aging periods, when compared with 0° and 30° counterparts. An increase in the diffusion coefficient caused an increase the activation energy. At 45° layering pattern, the activation energies of the JFMRLCs were higher. This layering pattern showed lower rate of composite degradation and higher service life. Lastly, Fick's law and Arrhenius principle were used to determine the degradation and maximum service life of the composites, considering the fiber orientation or layering patterns in the polymer matrix composites. Evidently, this current study has established that the jute fiber woven mat of 45° layering pattern is suitable for preparing polymer matrix composites for structural roof sheets, among other vital applications.

Compliance with Ethical Standards:

Funding: The authors wish to thank Kongu Engineering College and Kalasalingam Academy of Research and Education for providing the fabrication and testing facilities. The King Saud University authors acknowledge the funding from Researchers Supporting Project (RSP-2021/355), King Saud University, Riyadh, Saudi Arabia.

Conflict of Interest: The authors declare that they have no conflict of interest.

Acknowledgement:

References

- [1] Thomas S. Paul S A. Pothan L A. Deepa B. Natural fibers: Structure, properties and applications. *Cellulose Fibers: Bio- and Nano-Polymer Composites*. 2011; 3-42.
- [2] Zhu W H. Tobias B C. Coutts R S P. Langfors G. Air-cured banana-fiber-reinforced cement composites. *Cem Concr Compos*. 1994; 16(1): 3–8.
- [3] Sathishkumar T P. Navaneethakrishnan P. Shankar S. Rajasekar R. Rajin N. Characterization of natural fiber and composites - A review. *J Reinf Plast Compos*. 2013; 32(19): 1457–1476.
- [4] Ku H. Wang H. A review on the tensile properties of natural fiber reinforced polymer composites. *Compos Part B-Eng*. 2011; 42: 856–873.
- [5] Belaadi A, Bezazi A, Bourchak M, Scarpa F. Tensile static and fatigue behavior of sisal fibers. *Mater Des*. 2013; 46:76–83.
- [6] Dhakal H N. Zhang Z Y. Effect of water absorption on the mechanical properties of hemp fiber reinforced unsaturated polyester composites. *Compos Sci Technol*. 2007; 67: 1674–1683.
- [7] Carra G. Carvelli V. Long-term bending performance and service life prediction of pultruded Glass Fiber Reinforced Polymer composites. *Compos Struct*. 2015; 127: 308–315.
- [8] Rajeshkumar G. Hariharan V. Sathishkumar T P. Fiore V. Scalici T. Synergistic effect of fiber content and length on mechanical and water absorption behaviors of Phoenix sp. fiber-reinforced epoxy composites. *J Ind Text*. 2017; 47(2): 211-232.

- [9] Sathishkumar T P. Naveen J. Navaneethakrishnan P. Satheeshkumar S. Rajini N. Characterization of sisal/cotton fiber woven mat reinforced polymer hybrid composites. *J Ind Text.* 2017; 47 (4): 429-452.
- [10] Sahadat H M. Sarwaruddin C A M. Ruhul K A. Effect of disaccharide, gamma radiation and temperature on the physico-mechanical properties of jute fabrics reinforced unsaturated polyester resin-based composite. *Rad Effects Def Solids.* 2017; 172: 1–14.
- [11] Di B G. Fiore V. Valenza A. Effect of areal weight and chemical treatment on the mechanical properties of bidirectional flax fabrics reinforced composites. *Mater Des.* 2010; 31: 4098–4103.
- [12] Anna D K F. Aiswarya B. Hong B. Guijun X Sabu T. Effect of surface modification of jute fiber on the mechanical properties and durability of jute fiber-reinforced epoxy composites. *Polym Compos.* 2018; 39: E2519–E2528.
- [13] Dhakal H N. Zhang Z Y. Richardson M O W. Effect of water absorption on the mechanical properties of hemp fiber reinforced unsaturated polyester composites. *Compos Sci Technol.* 2007; 67: 1674–1683.
- [14] Yoldas S. Innovative multifunctional siloxane treatment of jute fiber surface and its effect on the mechanical properties of jute/thermoset composites. *Mater Sci Eng A.* 2009; 508: 247–252.
- [15] Guduri B R. Rajulu A V. Luyt A S. Effect of alkali treatment on the flexural properties of hildegardia fabric composites. *J Appl Polym Sci.* 2006; 102: 1297–1302.
- [16] Dimo H. Laura W. Pedram S. Long-term tensile properties of natural fiber-reinforced polymer composites: Comparison of flax and glass fibers. *Compos Part B.* 2016; 95: 82–95.
- [17] Rupesh K M. Rahul K S. Rajesh P. Roopesh Sinha. Natural fiber reinforced composite materials: Environmentally better life cycle assessment – A case study. *Mater Tod Proc.* 2020; 26(02): 3157-3160.

- [18] Leman Z. Sapuan S M. Saifol A M. Maleque M A. Ahmad M M H M. Moisture absorption behavior of sugar palm fiber reinforced epoxy composites. *Mater Des.* 2008; 29: 1666–1670.
- [19] Fiore V. Di Bella G. Valenza A. The effect of alkaline treatment on mechanical properties of kenaf fibers and their epoxy composites. *Compos Part B.* 2015; 68: 14–21.
- [20] Mansor M R. Mastura M T. Sapuan S M. Zainudin A Z. The environmental impact of natural fiber composites through life cycle assessment analysis. *Woodhead Publishing Series in Compos Sci Eng.* 2019; 257-285.
- [21] Saad M A. Adrian P. Aaron M T. Justin L. The effect of alkali treatment mechanical properties of kenaf fiber epoxy composite. *Key Eng Mater.* 2011; 471-472: 191-196.
- [22] Vivek M, Sandhyarani B. Physical and mechanical properties of bi-directional jute fiber epoxy composites. *Proc Eng.* 2013; 51: 561 – 566.
- [23] Athijayamania A. Thiruchitrambalamb M. Natarajana U. Pazhanivel B. Effect of moisture absorption on the mechanical properties of randomly oriented natural fibers/polyester hybrid composite. *Mater Sci Eng A.* 2009; 517: 344–353.
- [24] Dhakal H N. Zhang Z Y. Bennett N. Lopez-Arraiza A. Vallejo F J. Effects of water immersion aging on the mechanical properties of flax and jute fiber biocomposites evaluated by nanoindentation and flexural testing. *J Compos Mater.* 2014; 48(11): 1399–1406.
- [25] Venkateshwaran N. Elaya P A. Alavudeen A. Thiruchitrambalam M. Mechanical and water absorption behaviour of banana/sisal reinforced hybrid composites. *Mater Des.* 2011; 32: 4017–4021.
- [26] Dhakal H N. Zhang Z Y. Richardson M O W. Effect of water absorption on the mechanical properties of hemp fiber reinforced unsaturated polyester composites. *Compos Sci Technol.* 2007; 67: 1674–1683.

- [27] Rui-Hua H. Min-young S. Jae-Kyoo L. Moisture absorption, tensile strength and microstructure evolution of short jute fiber/polylactide composite in hygrothermal environment. *Mater Des.* 2010; 31: 3167–3173.
- [28] Gao M. Libo Y. Wenkai S. Deju Z. Liang H. Bohumil K. Effects of water, alkali solution and temperature aging on water absorption, morphology and mechanical properties of natural FRP composites. *Compos Part B-Eng.* 2018; 153:398-412.
- [29] Khiari R. Mhenni M F. Belgacem M N. Mauret E. Chemical composition and pulping of date palm rachis and *Posidonia oceanica* – a comparison with other wood and non-wood fiber sources. *Biores Technol.* 2010; 101: 775–80.
- [30] Sathishkumar T P. Naveen J. Satheeshkumar S. Hybrid fiber reinforced polymer composites - a review. *J Reinf Plast Compos.* 2014; 33(5): 454–471.
- [31] Carra G. Carvelli V. Aging of pultruded glass fiber reinforced polymer composites exposed to combined environmental agents. *Compos Struct.* 2013; 108: 1019–1026.
- [32] Sreekumarn P A. Agoudjil B. Boudenne A. Unnikrishnan G. Ibos L. Fois M. Thomas S. Transport properties of polyester composite reinforced with treated sisal fibers. *J Reinf Plas Compos.* 2011; 31(2): 117–127.
- [33] Sathishkumar T P. Navaneethakrishnan P. Shankar S. Kumar J. Mechanical properties of randomly oriented snake grass fiber with banana and coir fiber-reinforced hybrid composites. *J Compos Mater.* 2012; 47: 2181-2191.
- [34] Ridzuan M J M. Abdul Majid M S. Afendi M. Azduwin K. Amin N A M. Zahri J M. Gibson A G. Moisture absorption and mechanical degradation of hybrid *Pennisetum purpureum*/glass–epoxy composites. *Compos Struct.* 2016; 141:110–116.
- [35] Wambua P. Ivens J. Verpoest I. Natural fibers: can they replace glass in fiber reinforced plastics. *Compos Sci Technol.* 2003; 63: 1259–64.

Figures

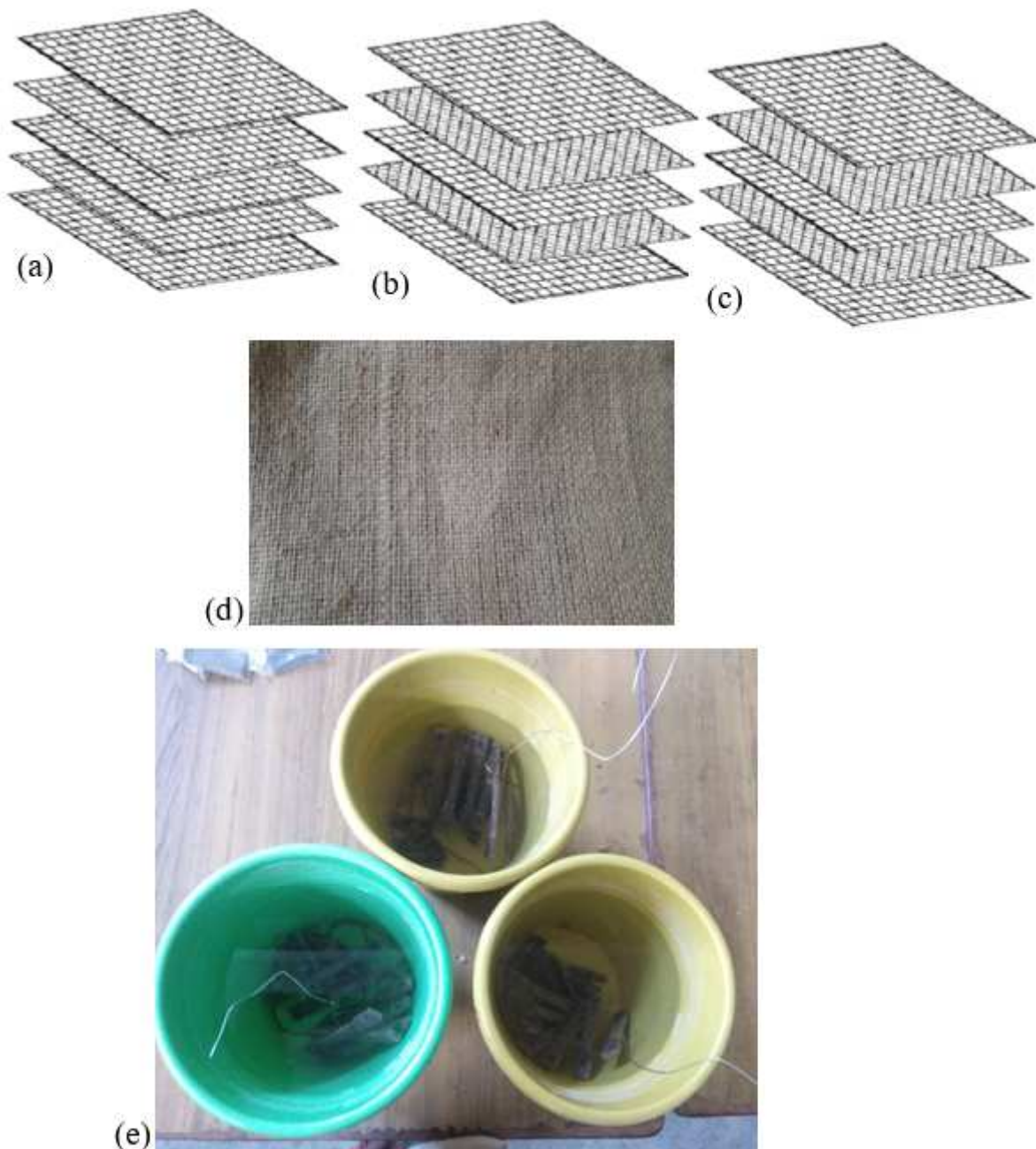


Figure 1

(a) Schematic jute fiber yarn mats, showing (a) $[0^\circ/0^\circ/0^\circ/0^\circ/0^\circ]$, (b) $[0^\circ/-30^\circ/0^\circ/+30^\circ/0^\circ]$, (c) $[0^\circ/45^\circ/0^\circ/45^\circ/0^\circ]$ layering patterns, (d) jute fiber yarn mat sample and (e) aging process of JFMRLCs.

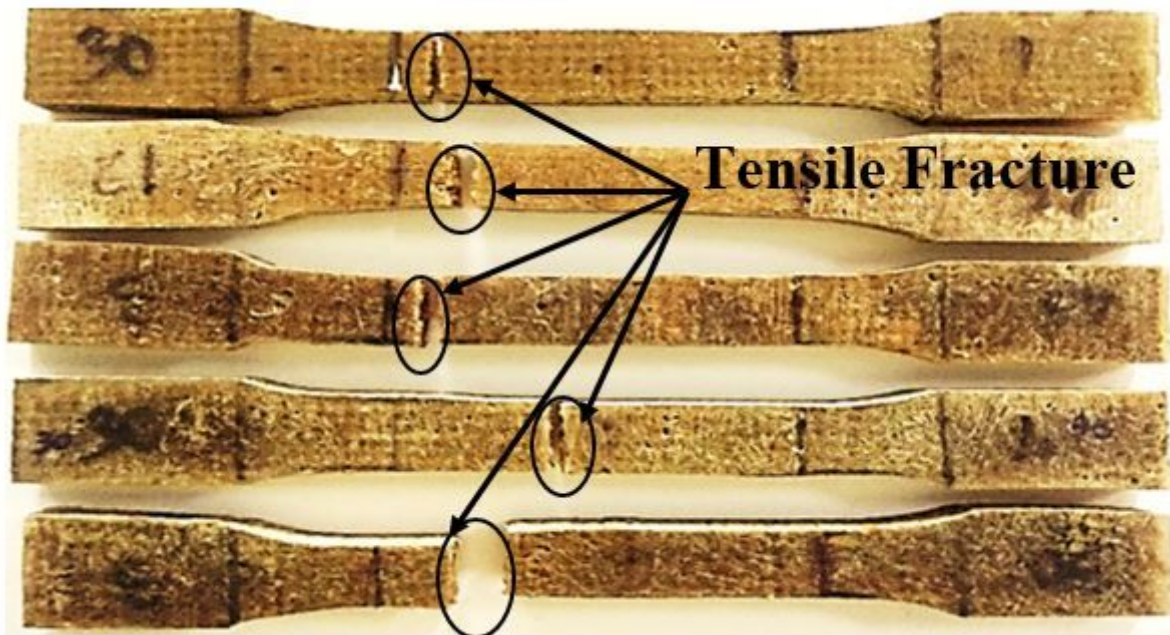


Figure 2

Tensile fractured samples.

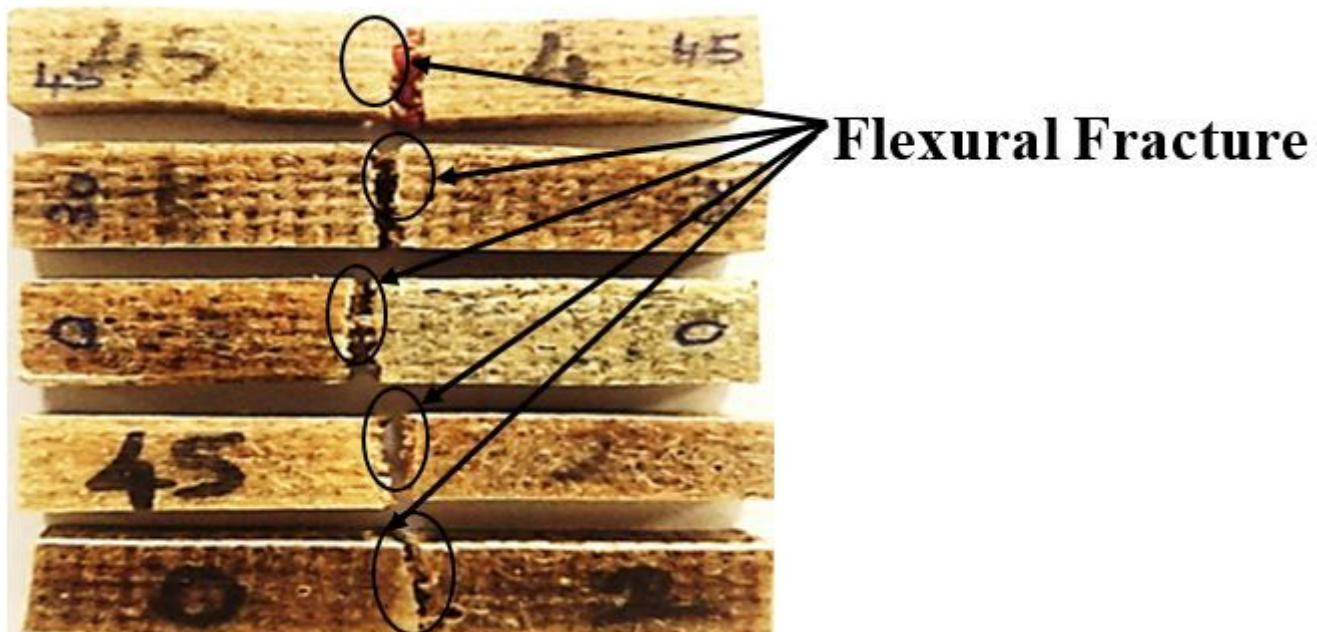
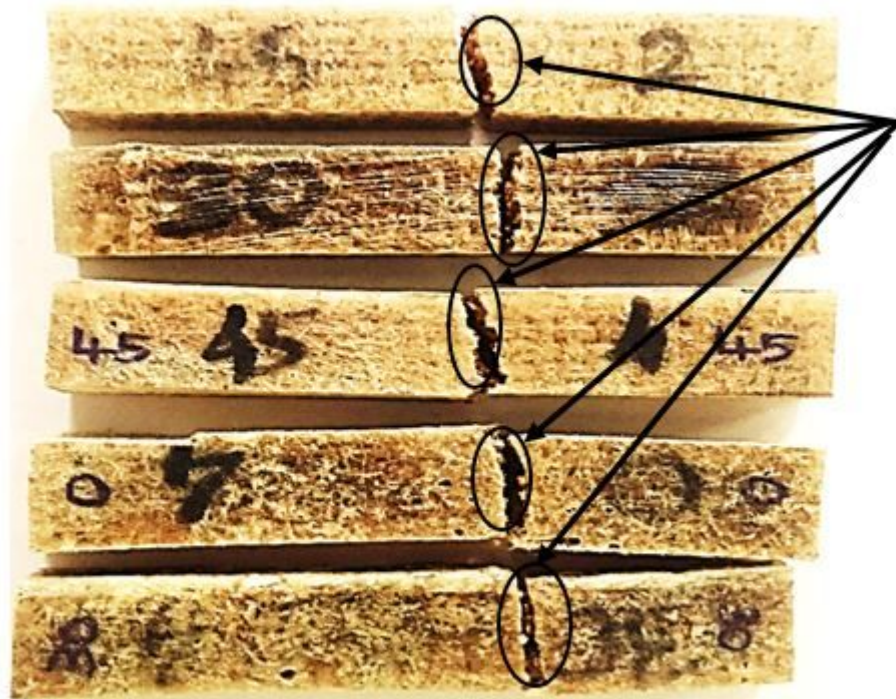


Figure 3

Flexural fractured samples.



Impact Fracture

Figure 4

Impact fractured samples.

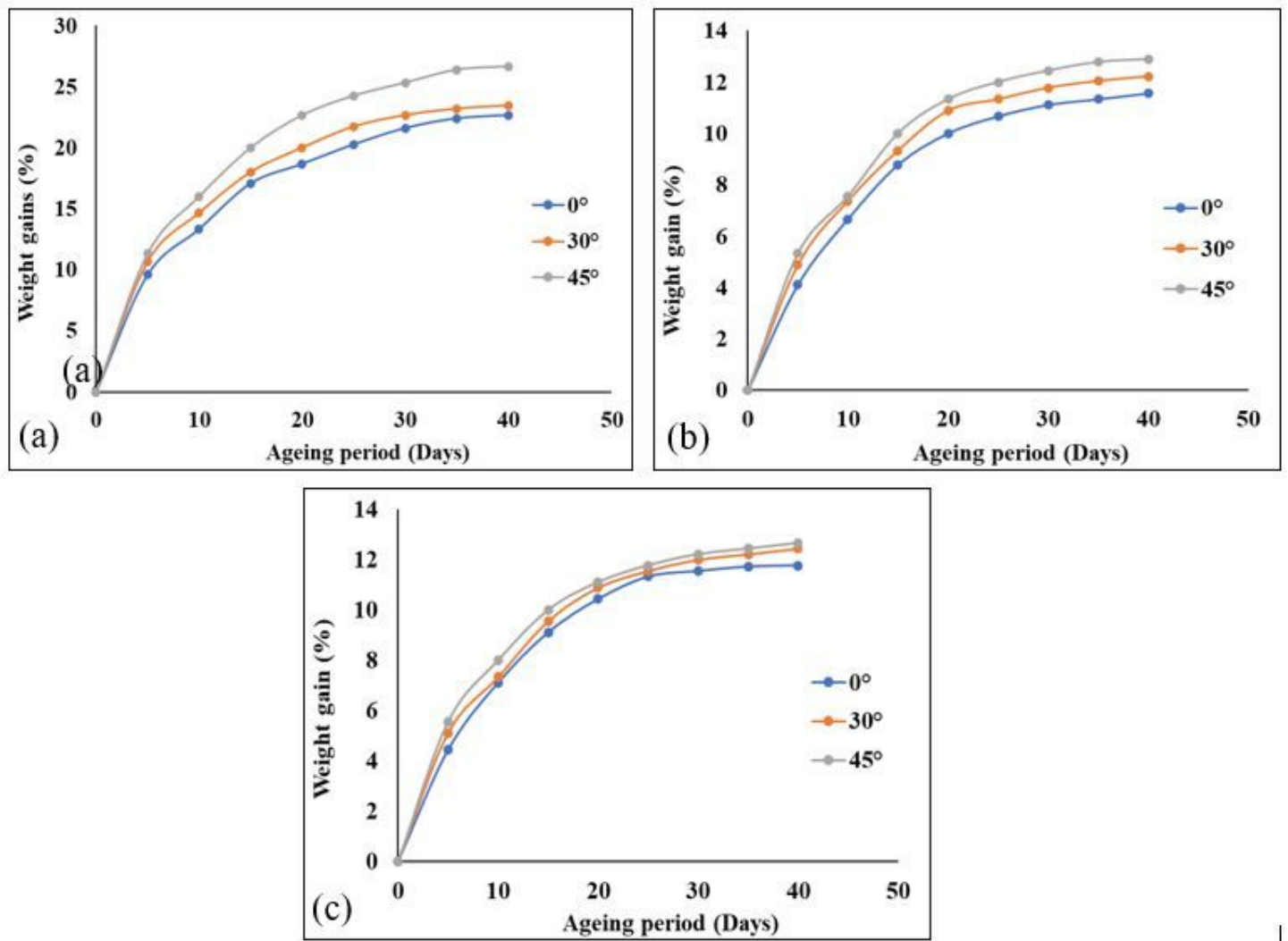


Figure 5

Weight gains by (a) tensile (b) flexural and (c) impact JFMRLC test samples.

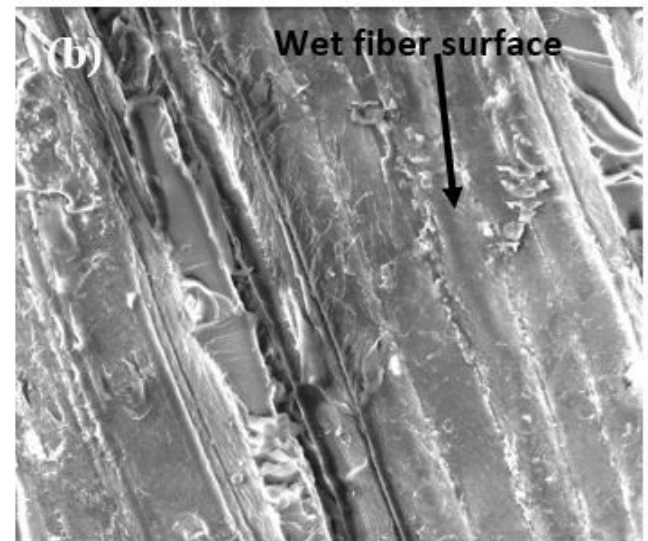
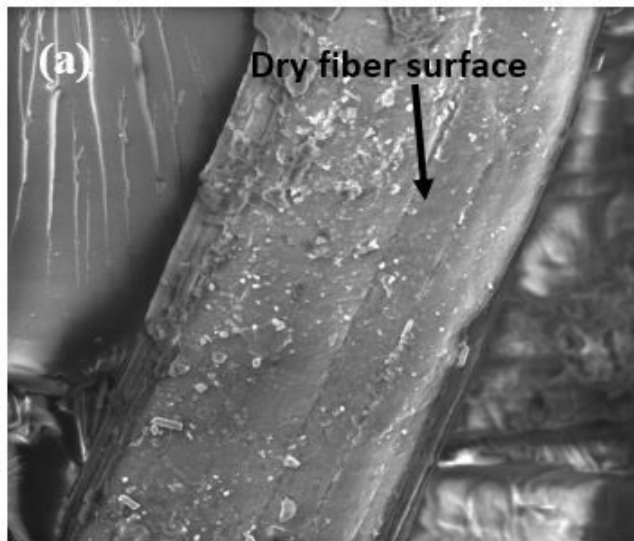


Figure 6

(a) Dry and (b) wet fiber surfaces.

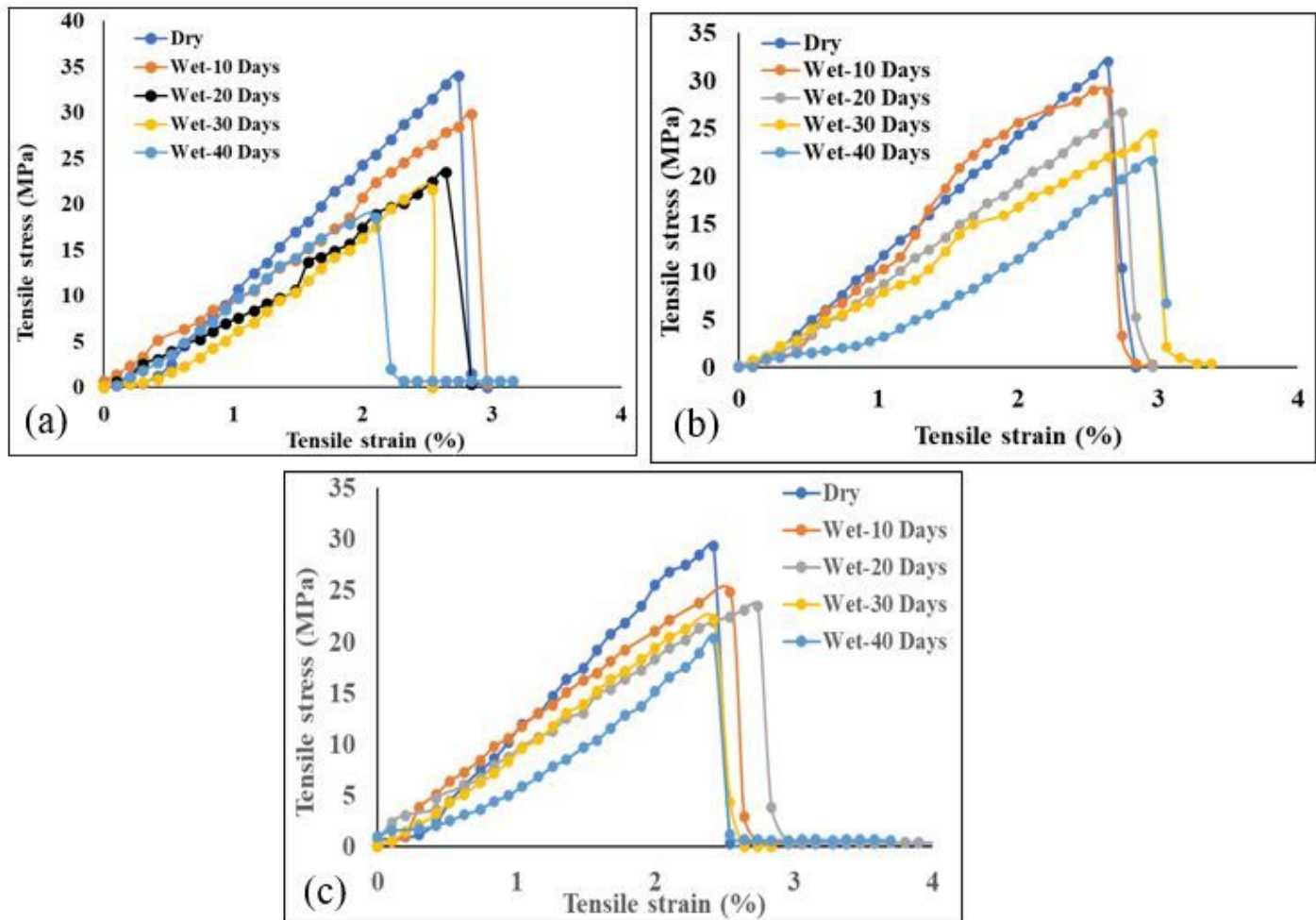


Figure 7

Tensile stress versus tensile strain curves of JFMRLCs at different periods for different layering patterns of (a) 0°, (b) 30° and (c) 45°

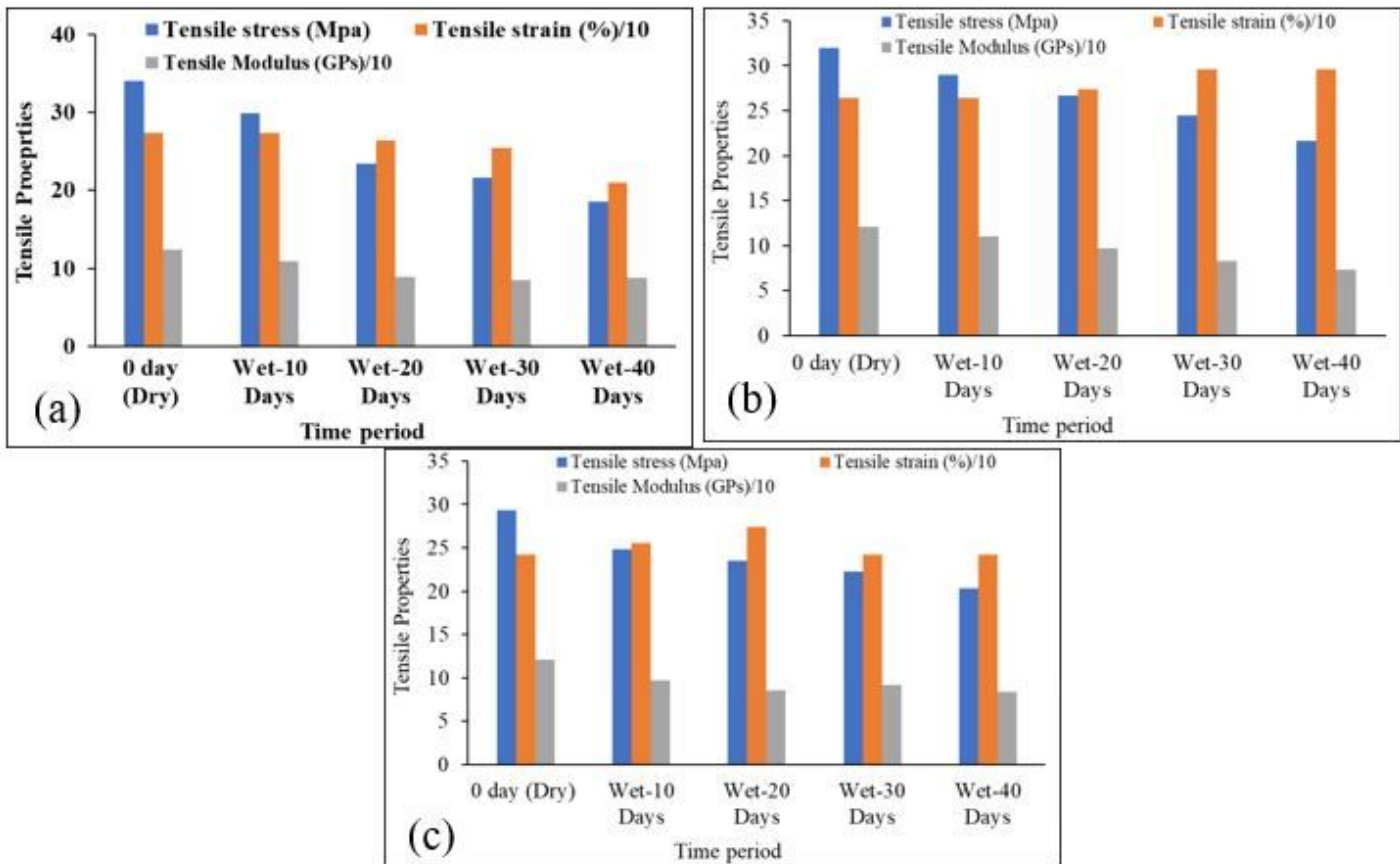


Figure 8

Tensile properties of JFMRLCs at different aging periods and layering patterns of (a) 0°, (b) 30° and (c) 45°.

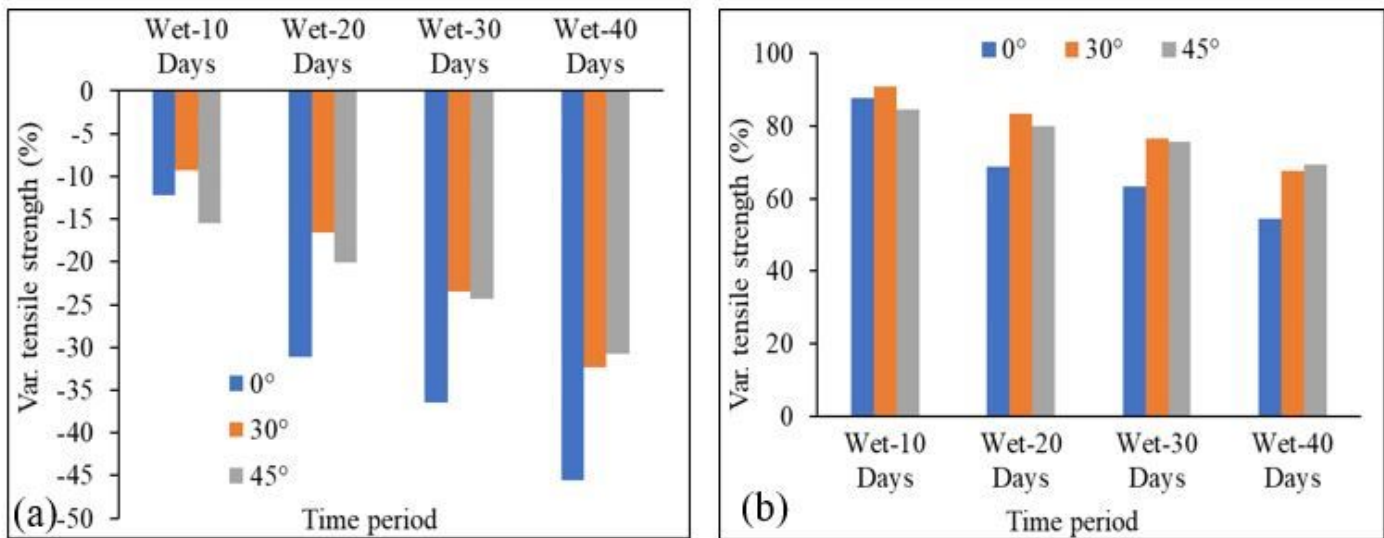


Figure 9

Tensile strengths (a) reduction and (b) retention of JFMRLCs at different aging periods and layering patterns.

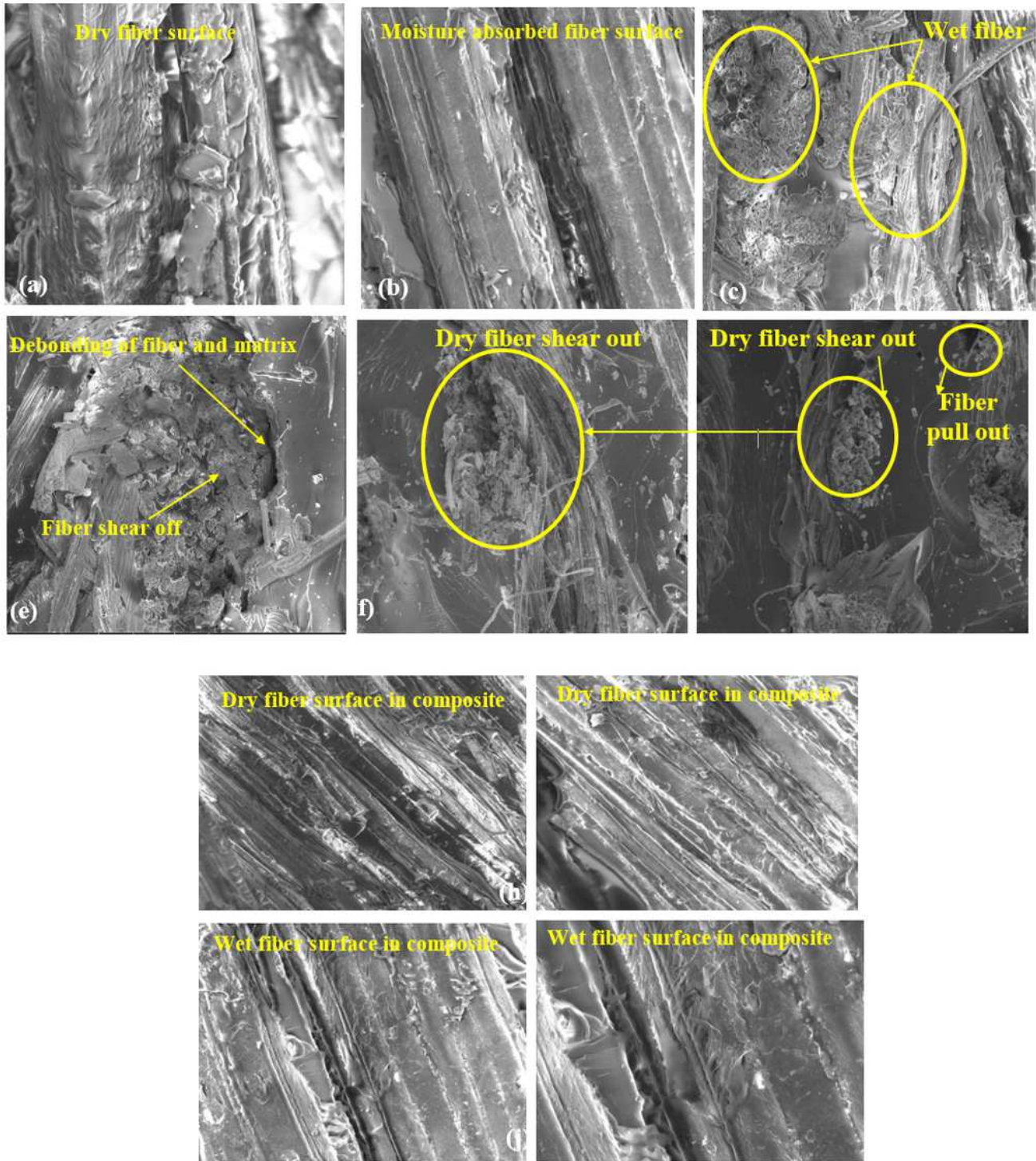


Figure 10

SEM images of tensile fractured surfaces of JFMRLCs with (a-f) 0° and (g-j) 30° layering patterns.

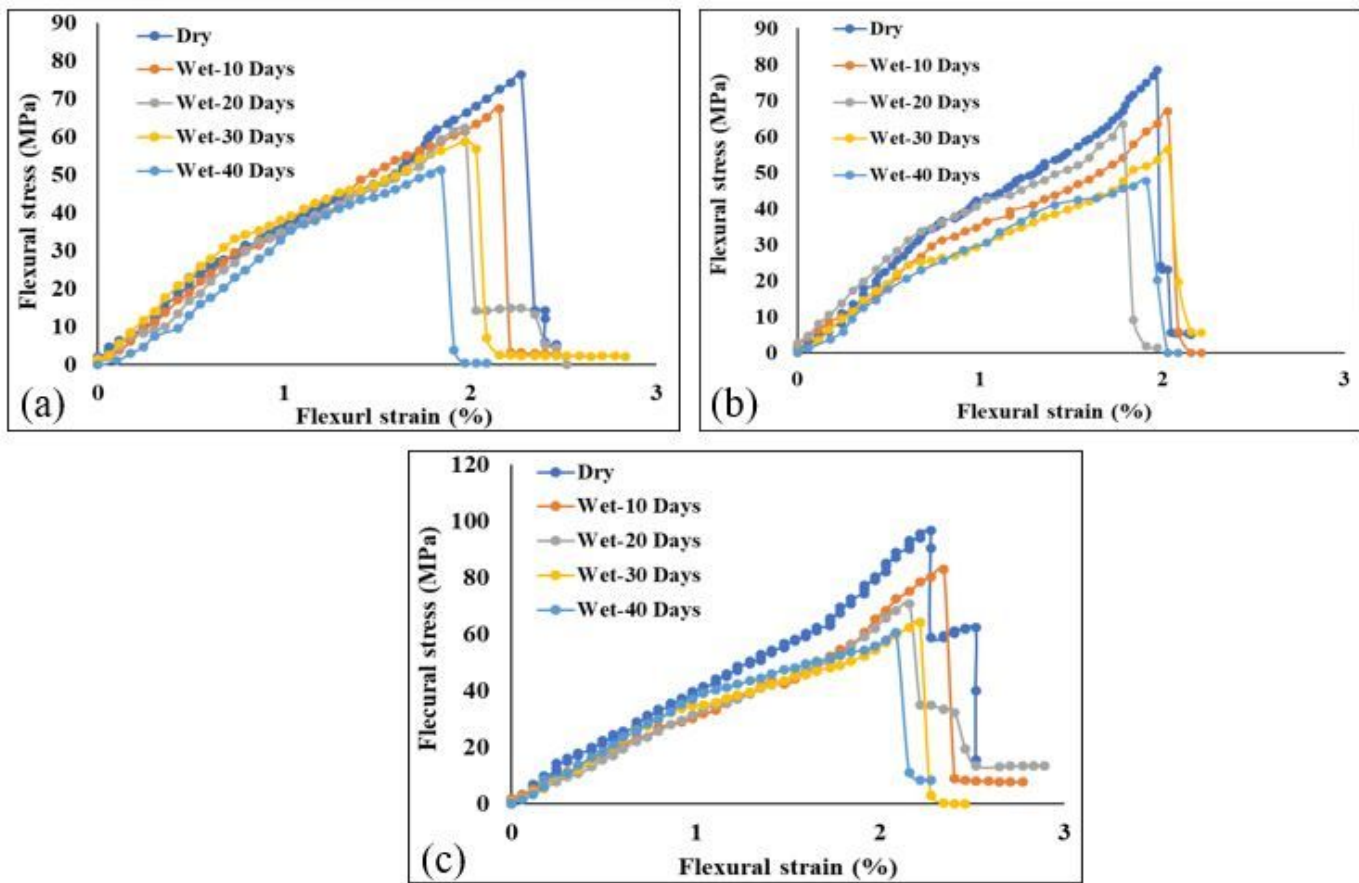


Figure 11

Flexural stresses versus flexural strains of JFMRLCs at different aging periods and layering patterns.

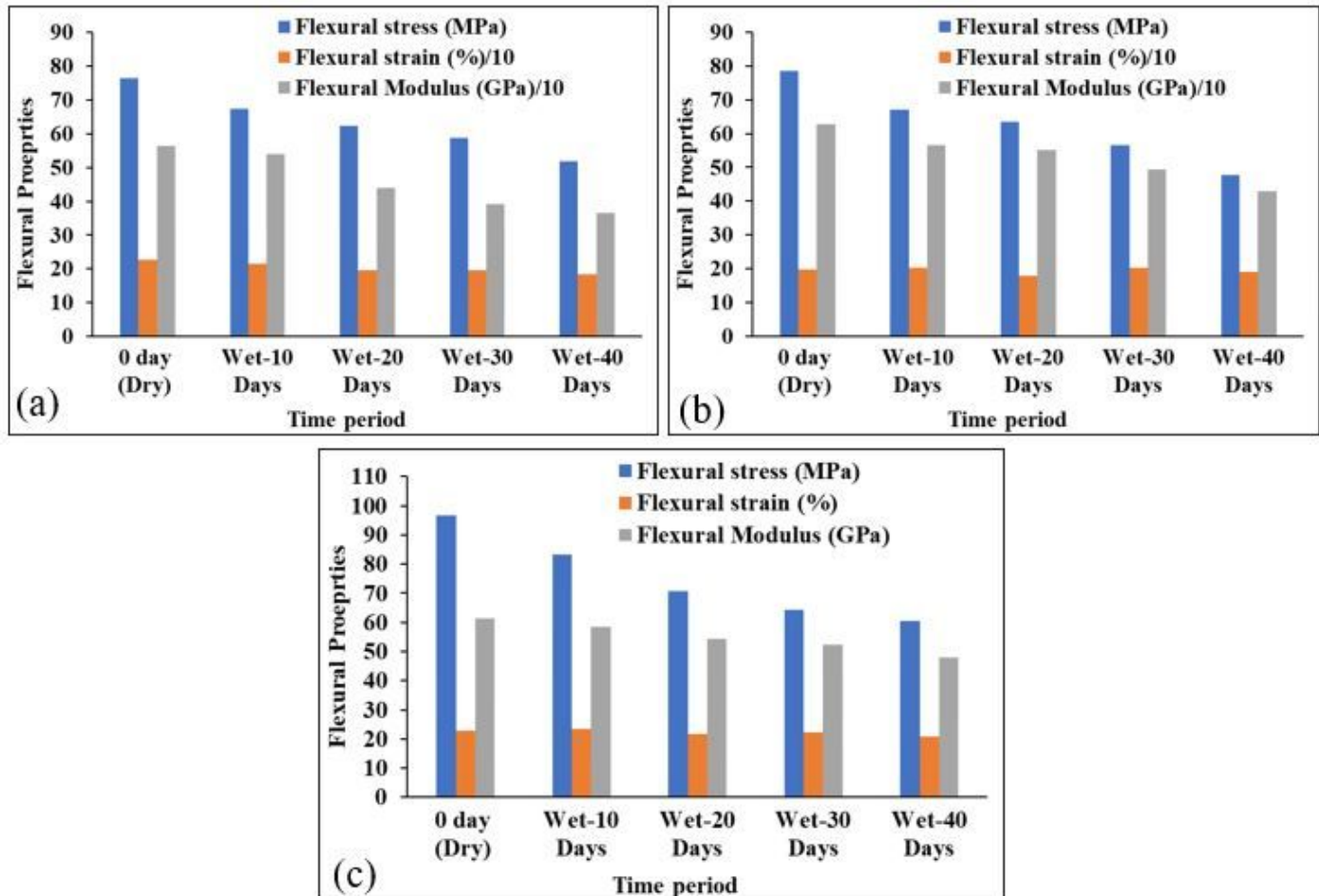


Figure 12

Flexural properties of JFMRLCs at different aging periods and layering patterns of (a) 0°, (b) 30° and (c) 45°.

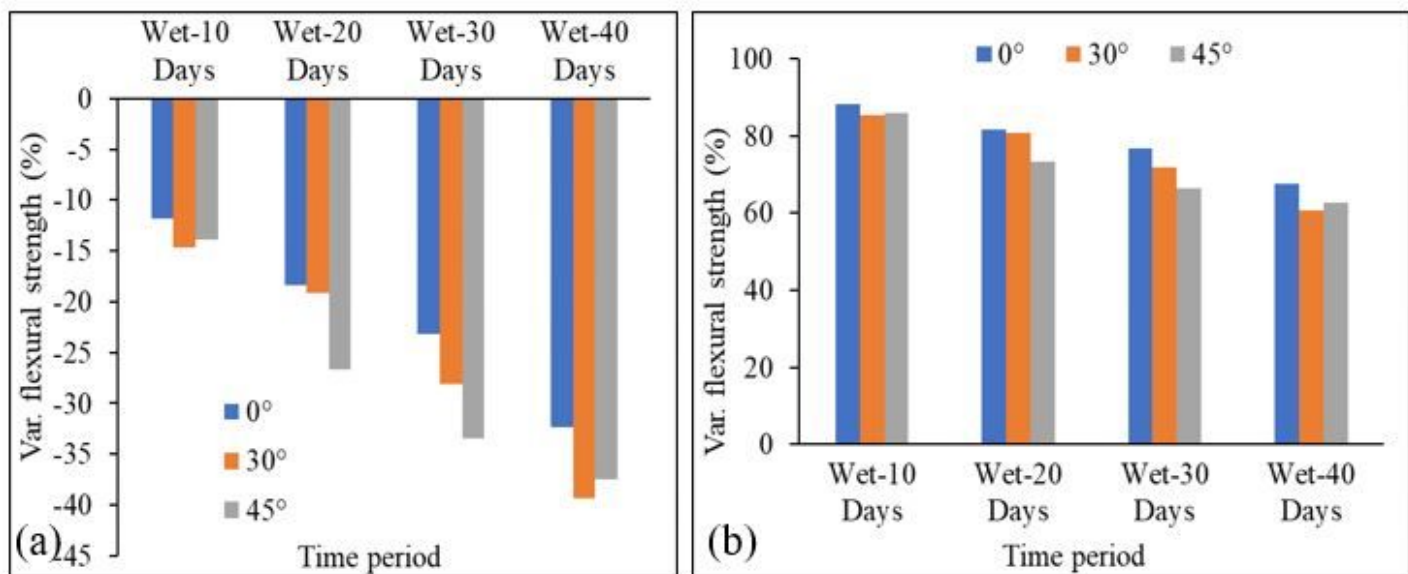


Figure 13

Flexural strengths (a) reduction and (b) retention of the various JFMRLCs at different aging periods and layering patterns.

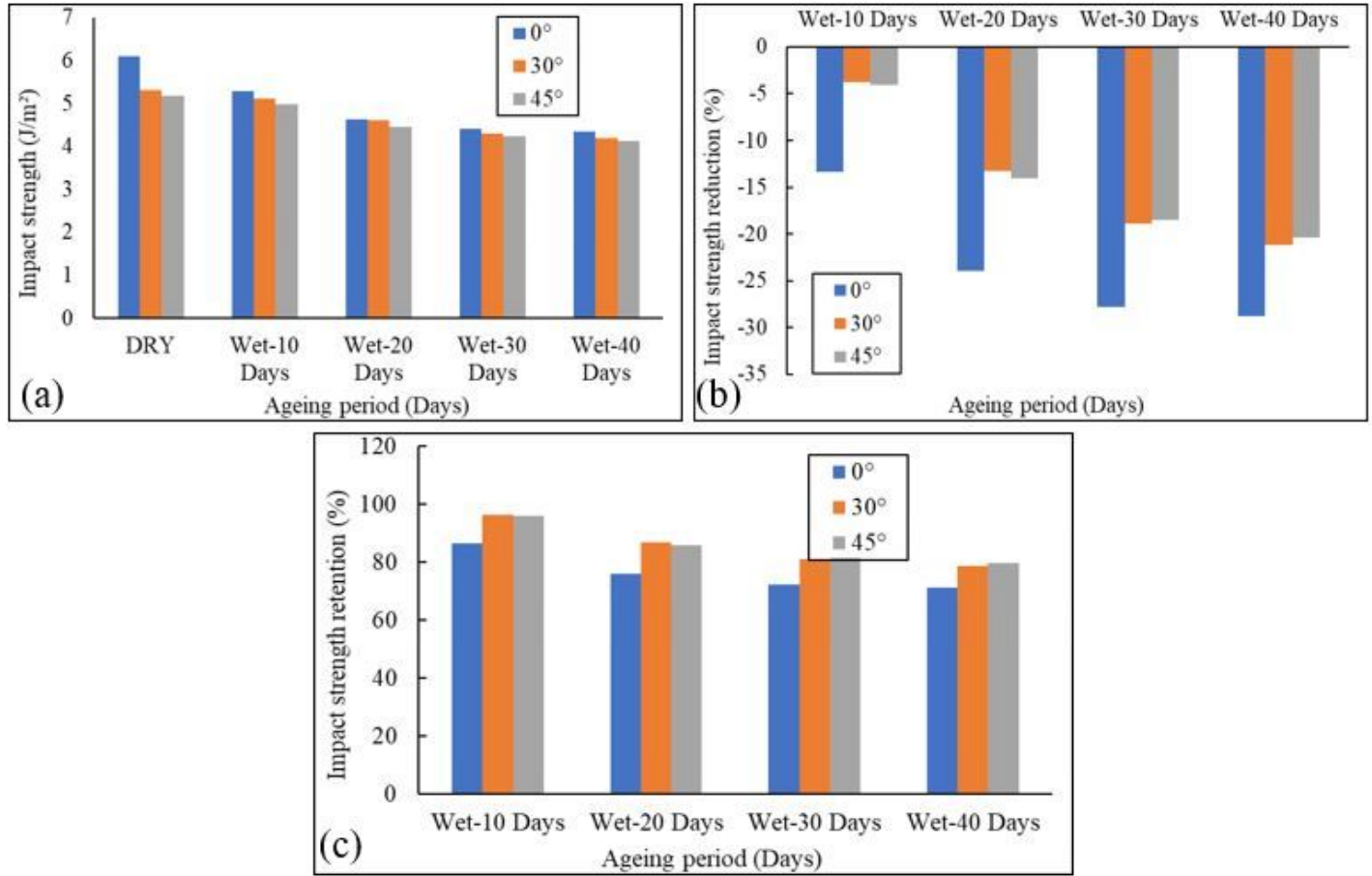


Figure 14

(a) Impact properties of JFMRLCs, showing their (a) strengths, (b) strengths reduction and (c) strength retention at different aging periods and layering patterns.

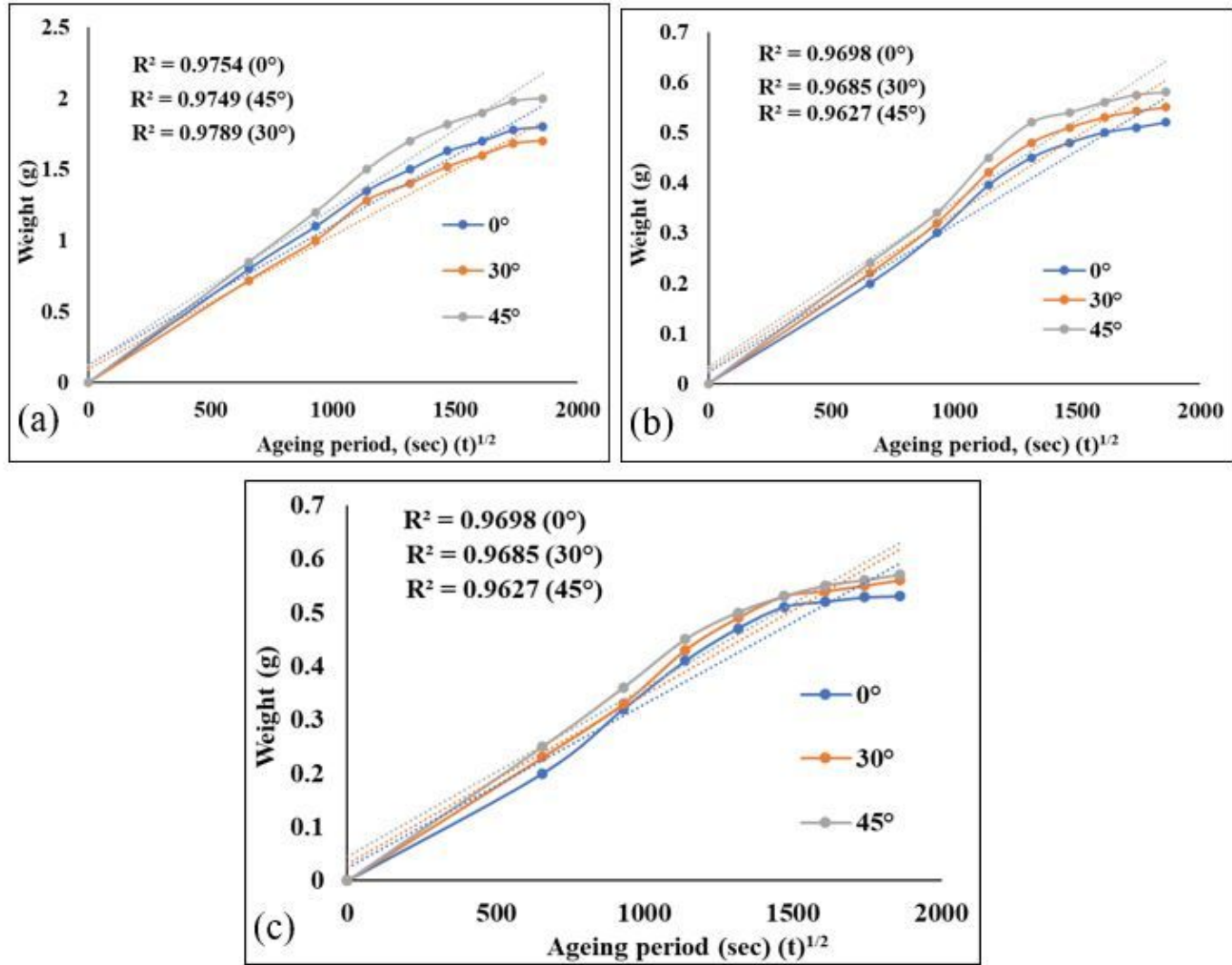


Figure 15

Weight gains versus square root of aging periods for prediction of diffusion coefficients of (a) tensile, (b) flexural and (c) impact samples.